



Stockholm
University

Bachelor Thesis

Degree Project in
Marine Geology 15 hp

Grain size analysis of a short sediment core from the Lomonosov Ridge, central Arctic Ocean

César Fuentes Guerrero



Stockholm 2015

Department of Geological Sciences
Stockholm University
SE-106 91 Stockholm

Abstract

Trigger core 07, is a 53 cm long sediment core that was collected during the Danish-Swedish expedition "Lomonosov Ridge off Greenland 2012" on the slope of the Lomonosov Ridge in the Arctic Ocean at a depth of 2522 m. This part of the world has experienced critical environmental changes during the Quaternary. Ice-sheets have advanced and retreated, and deposited sediments through all the Arctic Ocean. Glacial sediments contain coarser material and are gray, whereas interglacial sediments are brown, because of high amounts of manganese, and consist of fine-grained material. The aim of this project is to make grain size analysis on TC 07 with the purpose to make an interpretation of the grain size data in relation to glaciation history and paleo-oceanography. For that, a correlation with piston core 07 has been made, and also a correlation between piston core 07 and the Arctic Coring Expedition, ACEX.

The results showed that fine-grained material is more abundant in the top brown unit down to 32 cm, suggesting an interglacial period. This is followed by a gray-beige unit that goes down to 49 cm, and consist of coarser material, indicating glacial deposits. This unit can be linked to the Marine Isotope Stage 2, MIS 2, which began approximately 29000 years ago and ended about 14000 years ago

Sammanfattning

"Trigger core 07" är en 53 cm lång sedimentkärna som togs upp på ett djup av 2522 m från Lomonosovryggen i Arktisk under en dansk-svensk expedition kallad "Lomonosov Ridge off Greenland 2012". Den här delen av världen har genomgått kraftiga klimatförändringar under kvartär. Istäcken har vuxit fram och dragit sig tillbaka och avsatt sediment över hela Arktis. Sediment avsatta under istider, kännetecknas av att vara gråa med mycket grovt material, medan sediment avsatta under mellanistider är bruna, vilket är på grund av de höga halterna av mangan och består av finkornigt material. Målet med denna uppsats är att göra en kornstorleksanalys på sedimentkärnan, med syfte i åtanke på att göra en tolkning av informationen i förhållande till istidshistorik och paleo-oceanografi. För att kunna gå tillväga med det, har en korrelation gjorts mellan kärnan och "piston core 07", samt en korrelation mellan "piston core 07" och "Arctic Coring Expedition, ACEX".

Resultaten visar en brun enhet rik på finkornigt material ned till 32 cm, vilket är typiskt för mellanistider. Den följs av en grå-beige enhet som sträcker sig ned till 49 cm och består av grovkornigt material vilket tyder på istid. Den här enheten kan kopplas till "Marine Isotope Stage 2, MIS ", som varade mellan 14000 och 29000 år sedan.

Table of Contents

Abstract/Sammanfattning	2
1 Introduction	4
1.1 Purpose of the project.....	5
1.2 Background and Previous studies of the Arctic Ocean	5
1.3 Geology of the Arctic and the Lomonosov Ridge	6
1.4 Chronology	6
2 Methodology	7
2.1 Core description	7
2.2 Subsampling	8
2.3 Wet sieving	8
2.4 Drying	8
2.5 Malvern grain size analysis on the sieved samples	8
2.6 Malvern grain size analysis direct on the Sediment core.....	9
2.7 Grain Size.....	9
2.8 Core correlations	10
3 Results	10
3.1 Sieved sampling results	10
3.2 Bulk analysis	12
3.3 Grain Size results in Piston core 07.....	13
3.4 Correlation of TC 07 and PC 07	14
3.5 Correlation of PC 07 and ACEX	15
4 Discussion	16
4.1 Methodology	16
4.2 Sieved sampling analysis	16
4.3 Bulk analysis	17
4.4 Chronology of TC 07	17
5 Conclusions	18
6 Acknowledgements	19
7 References	19
7.1 Articles.....	19
7.2 Books	21
7.3 Internet references	21
8 Appendix	21

1 Introduction

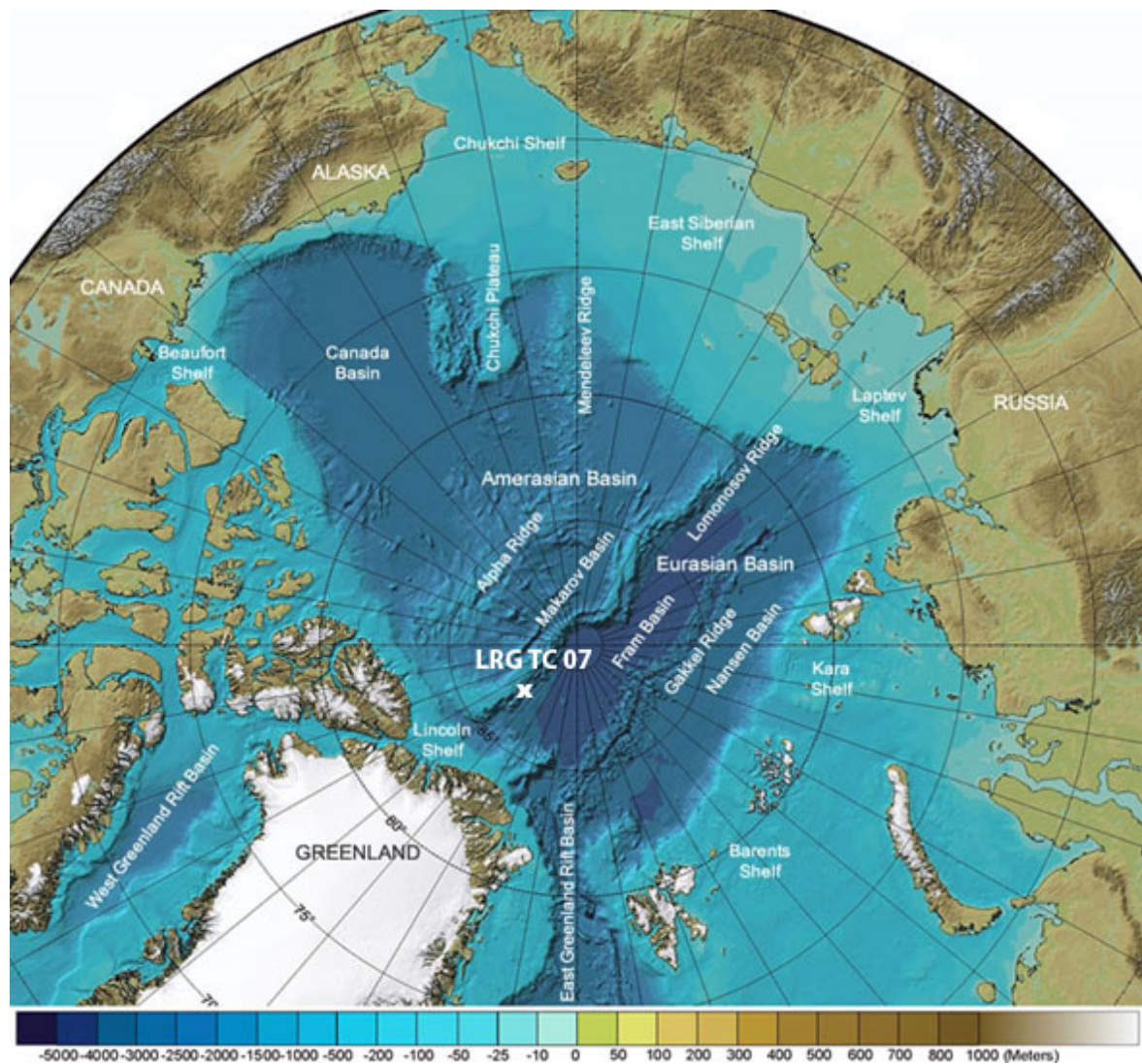


Figure 1, The map shows the Bathymetry of the Arctic Ocean. The North Pole is located in the middle of the map. Image modified from geology.com/articles/arctic-ocean-features, and created by Martin Jakobsson.

On July 31, 2012, aboard the icebreaker, Oden, the expedition of “Lomonosov Ridge off Greenland 2012” (LOMROG III) took off from Longyearbyen, Svalbard. The expedition ended at the same location on September 14 (LOMROG III- Cruise Report). The Danish-Swedish cooperation was 80% financed by the Continental Shelf Project of the kingdom of Denmark and 20% by the Swedish Polar Research Secretariat (LOMROG III- Cruise Report). Three science projects, which were sediment coring, microbial communities, and plankton ecology, was the Swedish part of the cruise. The science project of sediment coring, PAWS (Paleoceanography of the Arctic- Water masses, Sea ice, and sediments) collected 10 piston cores and 11 trigger weight cores extracting a total amount of 61 meters of sediments. The aim of the science project was to gain knowledge of the critical role of climate from about 125000 years (Eemian Interglacial) to present (LOMROG III-Cruise Report). Trigger weight core 07, which is the core this study is going to focus on, was collected on August 15 at a depth of 2522 meters on the slope of the Lomonosov ridge at the location $88^{\circ}11'51.5N$ and $55^{\circ}41'04.3 W$ together with piston core 07 (LOMROG III-Cruise Report).

1.1 Purpose of the project

The purpose of the study is to measure and interpret grain size data on trigger weight core 07 from the slope of the Lomonosov Ridge in the central Arctic Ocean (fig. 2). The grain size data is compared and correlated to density and grain size data from other sediment cores (Piston core 07 and the Arctic Coring Expedition, ACEX) from the Lomonosov Ridge and the Arctic Ocean. An interpretation of the grain size data in relation to glaciation history and paleo-oceanography is made.

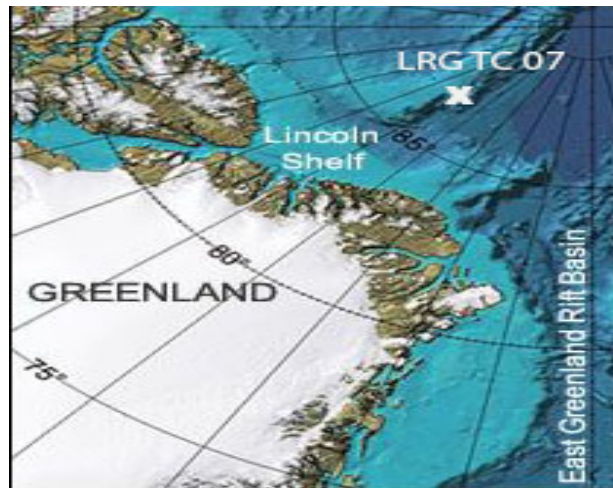


Figure 2. The location of where Trigger weight core 07 was collected on the Lomonosov Ridge. Image modified from geology.com/articles/arctic-ocean-features.

1.2 Background and Previous studies of the Arctic Ocean

In recent years, the knowledge of the Arctic Ocean has increased with the recovery and study of sediment cores from different parts of the Arctic Ocean.

The Arctic Ocean (fig.1) is surrounded by the Canadian Arctic islands, Greenland, and the North American craton in the western hemisphere, and at the eastern hemisphere it is surrounded by the Baltic Shield, Barents Shelf, and the Siberian continental shelf (fig.1) (Shephard *et al.*, 2013). It has only one deep-water connection to the world's oceans, and it is via the Fram Strait (Jakobsson *et al.*, 2008) between Svalbard and Greenland. Ice initiation began approximately 46 million years ago in the Arctic Ocean (St. John, 2008).

No other ocean has experienced such dramatic changes (both physiographic and environmental) through the Quaternary as the Arctic Ocean (Jakobsson *et al.*, 2014). During the Quaternary period, has ice-sheets advanced and retreated across the Arctic margins (Strand & Immonen, 2010), as well as in other parts of the world. These series of ice-sheets advance and retreat are related to glacial-interglacial cycles (Strand & Immonen, 2010). During the “Last Glacial Maximum”, LGM, 26500-19000 years ago, ice-sheets reached their maximum extent around the World (Clark *et al.*, 2009). Nowadays is the perennial ice cover in the Arctic comprised of sea ice and smaller amounts of glacial ice (Jakobsson *et al.*, 2001). Ice-rafting icebergs and sea ice-rafted debris are the main sources for sediment to the Arctic Ocean (Jakobsson *et al.*, 2000), especially for the Lomonosov Ridge which gets its sediments from the Kara Sea and Laptev Sea areas (Sellén *et al.*, 2008 and references therein).

Determining glacial and interglacial periods are important for environmental studies. Glacial and interglacial periods are reflected in distinct ways from one another. Sediment texture, chemistry, color, and faunal-assemblages are proxies for determining glacial/interglacial periods (Jakobsson *et al.*, 2001 and references therein).

Interglacial sediments are generally bioturbated, fine-grained, and consistently dominated by silt and clay with low amounts of sea ice transported coarse-grained material (Jakobsson *et al.*, 2014). These sediments, display a dark brown color, owing it to an enrichment of manganese hydroxides (Löwemark *et al.*, 2014). Manganese, Mn, is an important indicator of interglacial periods, its input, transport and burial are controlled by different processes, which acts on both seasonal time scales and orbital time scales (Löwemark *et al.*, 2014).

During winter, the Mn flux is strongly reduced, whereas it reaches its highest input during spring (Hölemann *et al.*, 2005).

The manganese cycles are sensitive to environmental changes, especially to those occurring in the water column and riverine input (Jakobsson *et al.*, 2000; Löwemark 2014). Coastal erosion and riverine input are the main sources for Mn input to the Arctic Ocean (Macdonald and Gobeil, 2012; Löwemark *et al.*, 2014), during glacial periods when large ice-sheets blocks rivers from the sea and coastal erosion decreases, a remarkable reduction of Mn is noticeable. Rivers that drain out in the Arctic Ocean are enriched in Mn compared to the world river average due to peat bogs (Löwemark *et al.*, 2014 and references therein). Sediments deposited during glacial periods are mostly beige to gray in color. They are often depleted or have low amounts of Mn, have little or none microfossils and bioturbation, and they contain higher amounts of coarser grains (Jakobsson *et al.*, 2000). Glacial deposits show higher bulk density and higher P-wave velocity, in contrast to the lows in bulk density and P-wave velocity with peaks in the magnetic grain size proxy data, which commonly occurs in the dark brown, Mn enriched zones (O'Regan *et al.*, 2008).

1.3 Geology of the Arctic and the Lomonosov Ridge

The Lomonosov Ridge is about 1700-km-long, 20-70-km-wide with a mean deep of 2000 m (Timmermans *et al.* 2005), and stretches from Northern Greenland to the Laptev Sea shelf-off the New Siberian Islands (Björk *et al.*, 2007). It separates the two major bathymetric features in the Arctic Ocean, the Amerasian Basin and the Eurasian Basin (Shephard *et al.*, 2013) and therefore blocks deep-water exchange between these two basins (Björk *et al.*, 2007). These differences are reflected in the different properties of the water masses as the Amerasian Basin is warmer, less dense, and saltier (Björk *et al.*, 2007 and references therein).

The Lomonosov Ridge is made up by continental crust (~26 km thick), it detached from Barents-Kara Sea continental margin about 56 Ma (Minakov *et al.*, 2012). As it began to drift apart from Barents-Kara Sea continental margin, the Eurasian basin began to form due to a very slow spreading on the Gakkel Ridge (Minakov *et al.*, 2012), ~1 cm/year (Verzhbitskii *et al.*, 2012).

The Lomonosov Ridge has experienced erosion down to 1000 m (Jakobsson *et al.*, 2008). The origin of this erosion is under discussion. However, Jakobsson and co-authors (2008), suggest that coherent ice masses such as moving ice shelves grounded on these bathymetric highs.

1.4 Chronology

Creating age models in the Arctic Ocean has been difficult. That is because of the low sedimentation rates that generally are not higher than a few cm/1000 years in the central Arctic Ocean and in the Lomonosov Ridge (Backman *et al.*, 2004), the low biological productions and the strong oxygenation of bottom sediments that causes diagenetic alteration of biogenic material (Chanell and Xuan, 2009; Polyak *et al.*, 2013). This have also caused complications in the challenge to create age models that would allow detailed flux comparison through glacial and interglacial periods, as well as correlation with cores from different oceanographic settings (Backman *et al.*, 2004).

Attempting to correlate sediment cores through color description can also be complicated because of the change in color that can affect the cores when they are exposed to oxygen and laboratory conditions (Sellén *et al.*, 2008).

Lisiecki and Raymo (2005) presented in their paper, what they called the LR04 stack, which is an average of 57 globally distributed benthic $\delta^{18}\text{O}$ records collected from the scientific literature. The global ice volume and temperatures in deep-sea are two of the main parameters that influence the benthic $\delta^{18}\text{O}$ records. These records were put into an age model using a graphic correlation technique (Lorrain Lisiecki's homepage 2015). This age model, Marine Isotope Stages, or MIS, is used to correlate sediments in relation to age. MIS spans 5.3 million years, from MIS 1 (present day-14 ka) to MIS T66 (5315 ka).

In the summer of 2004, the expedition 302 of the Integrated Ocean Drilling Program (IODP), also known as the Arctic Coring Expedition (ACEX) recovered more than 400 m of sediment cores (ACEX preliminary report webpage, 2004) from four closely spaced sites on the Lomonosov Ridge (O'Regan *et al.*, 2008). The sediments provided a 27 m continuous section from the Lomonosov Ridge (O'Regan *et al.*, 2008). By using a multi-sensor core logger, MSCL, the ACEX cruise measured bulk density, P-wave velocity and magnetic susceptibility (O'Regan *et al.*, 2008) and correlated with the Marine Isotope Stages.

2 Methodology

2.1 Core description

LOMROG12-TC07, is a 53 cm long sediment core from the slope of the southwestern Lomonosov ridge (fig. 3). It can be divided into six units based on the sediment color and apparent contact between the different units.



Figure 3. The photo shows Trigger core 07. Photo taken by Richard Gyllencreutz.

The top unit, which is the one closest to the sea floor goes down to 32 cm. It is quite homogenous down to 10 cm with a very dark gray brown sandy clay, and it is followed by a 3 cm thick darker brown subunit with a finer grain size, possibly coarse silty clay. Between 13 cm and 27 cm a gradual change in color towards a more yellow brown is observed. This subunit show many dark colored (dark reddish brown) stripes and dots. The grain size of this part varies between fine size sandy clay and medium size sandy clay. From 27 cm down to 32 a brown homogenous subunit is observed with fine size sandy clay.

The second unit, which begins at 32 cm and is only 1 cm wide, shows sharp contact with unit 1 and unit 3. It is distinguish by light yellowish brown color. The grain size of this unit is medium size sandy clay.

At 33 cm a third unit is observed that goes down to 49 cm. The top 3 cm shows a light brown gray with fine size sandy clay. Between 36 cm and 49 cm a gradual change in color is observed.

The top show a darker olive brown than the bottom subunit. Many distinctive reddish brown stripes are observed, and between 44 cm and 45 cm a large one is present.

The grain size of this unit is fine sandy clay.

Between 49 cm and 53 cm, 3 different homogenous units can be observed.

All three have different distinctive colors. The top unit of these three, which lays between 49 cm and 51 cm is a homogenous dark grayish brown. It is followed by a cm-wide olive brown unit. This layer contains finer grains. The bottom unit is very dark brown with coarser grains than the overlying layer.

2.2 Subsampling

As the core was 53 cm long and the sampling was made with 1 cm interval, 53 samples were totally collected. The samples were put on weighing boats, which were weighed with sediment and without sediment for calculating the wt% after drying.

For the purpose of doing analysis on the grain size, finer particles ($<63 \mu\text{m}$) are separated from coarser particles ($>63 \mu\text{m}$), and it is done by wet sieving the samples before drying them (McManus, 1988). According to the author, clays and silts may produce crusts or durable pellets if the particles are not separated before drying.

2.3 Wet sieving

Before the wet sieving, the samples were put into 250 ml or 400 ml beakers. For the intention of getting all grains from the weighing boat into the beaker, a dispersion solution was used, approximately 50-100 ml of 0.5% sodiumhexametaphosphate solution, $(\text{NaPO}_3)_6$, Calgon, was used. The beakers were then put on a shaker table during the night.

For the sieving, a $63 \mu\text{m}$ sieve mesh and a 1000 ml beaker was used. Before the sieving, the samples were put in an ultrasonic bath with the intention of loosening possible particle aggregates. The samples were then loaded into the $63 \mu\text{m}$ sieve mesh and washed with 0.5% Calgon. The particles larger than $63 \mu\text{m}$ were put into weighing boats for drying.

2.4 Drying

The 1000 ml beaker (which contained the finer grains), was dried in an oven at 50°C and the plastic weighing boats with the coarser material in an oven at 40°C .

2.5 Malvern grain size analysis on the sieved samples

After drying the samples in the oven they were prepared for measurement using a Malvern grain size analyzer (fig. 4). The Malvern grain size analyzer works by measuring the intensity of light scattering as a laser beam goes through a dispersed particle sample. The scattered pattern that is created by the different sizes of the particles is calculated by the obtained data from the laser diffraction (Malvern Webpage 2015).

It was important to let the instrument “warm up” 30 minutes before using it.

After the “warm up”, the program “Mattersizer 3000” was opened. A cleaning of the system was next step, the cleaning was made with deionized water. Also, a control of the detectors was made were detector 1 needed to be <80 and detector 20 <20 , with the purpose to ensure that the system was clean. If it was clean the values of detector 1 to detector 60 would go from high to low. Following this, the magnetic stirrer set at 3500 rpm, was started, which is to keep the samples in suspension. The next step was to put the sample in. The ideal obscuration (depends on the amount of sample), which is the light intensity absorbed by the sample, should be between 5-15%, higher obscuration than that would give better representativeness, however, it could lead to multiple scattering.

Before putting the sample into the sample container, different methods were tested. The standard routine would be to put the dried sample directly into the sample container, with 3 ml 10% Calgon, and 3 minutes of pre-stirring in which the first minute it also was ultra-sounded. However, the results showed that the samples needed more time of stirrer and more time of ultra-sound. Therefore, after testing different methods, the ideal method was to put the dried samples into a small beaker and fill it up with 50 ml of deionized water and let it ultra-sound. Next step was to put the sample into the sample container and pour in 3 ml of 10% Calgon to prevent grain aggregation. By applying this method, the samples needed only 3 minutes of stirrer and 1 minute of ultra-sound. The instrument makes 5 measurements per sample.



Figure 4. The above photo shows the Malvern Mastersizer 3000 which was used for the grain size analysis. Photo taken by César Fuentes Guerrero.

2.6 Malvern grain size analysis direct on the Sediment core

For the purpose of comparison between two different approaches, samples were also taken directly from the sediment core. They were put into small beakers filled with deionized water and ultra-sounded before the Malvern grain size analysis began. The procedure was almost the same as with the dried samples, except that they were ultra-sounded during two minutes during the stirrer, which was for prevention particle aggregation as they were taking directly from the core.

2.7 Grain Size

The grain size results will be grouped into three different intervals, <2 μm , 2-63 μm , and >63 μm . Table 1, shows the classification for the different grain sizes that could be present in the sediments.

Table 1. Show the grain size classification of particles >2000 μm . (Based on ISO 14688-1)

		Size (μm)
Sand	Coarse	630-2000
	Medium	200-630
	Fine	63-200
Silt	Coarse	20-63
	Medium	6.3-20
	Fine	2-6.3
Clay		<2

2.8 Core correlations

To estimate the age of the sediments units in TC 07 in relation to MIS (Marine Isotope Stages), a correlation between the bulk analysis of $>63 \mu\text{m}$ and PC 07 core section 1 $>63 \mu\text{m}$ is needed. Both curves are going to be plotted on the same graph and lines are going to be drawn at points where they appear to be connected and represent the same tendency.

Following that, a correlation of the density curve for PC 07 and the ACEX density curve is going to be made, The same principle as in the correlation of TC 07 and PC 07 is going to be applied for the correlation of PC 07 and ACEX.

3 Results

3.1 Sieved sampling results

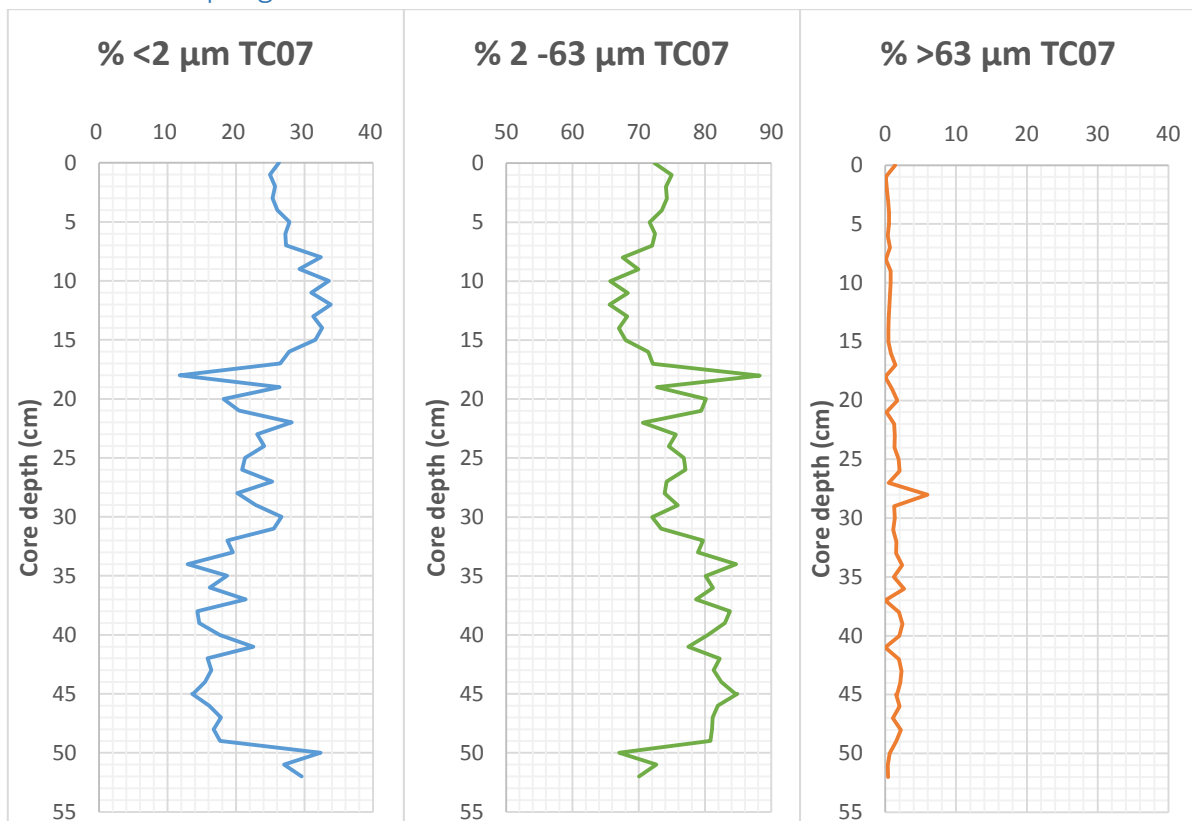


Figure 5. Results from the Malvern Grain Size analyzer over the sieved samples.

The three graphs (fig.5) show variations in concentration with core depth. The graph for $<2 \mu\text{m}$ follows an opposite tendency to the graph for grains between $2-63 \mu\text{m}$ whereas the third graph $>63 \mu\text{m}$, surprisingly is not 0 as it should be, instead it has several peaks, with the highest reaching almost 6%.

The highest concentration of grain size is between 2 and $63 \mu\text{m}$, where its highest concentration is ca. 88% and its lowest concentration is ca. 65%.

Down to core depth 16 cm, the curve do not show any major abrupt changes but a gradual decrease (following a small increase) in concentration occurs from the top of the core down to 6 cm. From 6 cm to 15 cm some fluctuations occur, but without significant changes.

From 17 cm down to 52 cm there are several abrupt changes. The largest variations are between 17 cm and 22 cm, and between 41 cm and 50 cm. At 17 cm, where the concentration is ca. 72% a significant increase occurs, and at 18 cm has the concentration reached almost 88%, before dropping to ca. 73% at 19 cm.

Following that, a pattern of fluctuations occur down to 49 cm, where an abrupt decrease in concentration is seen down to 50 cm (from ca. 81% to ca. 67%). At 51 cm, an increase in concentration occurs (to ca. 72%), whereas at 52 cm, which represent the bottom of the trigger core is the concentration ca. 70%.

3.2 Wt% > 63 μm

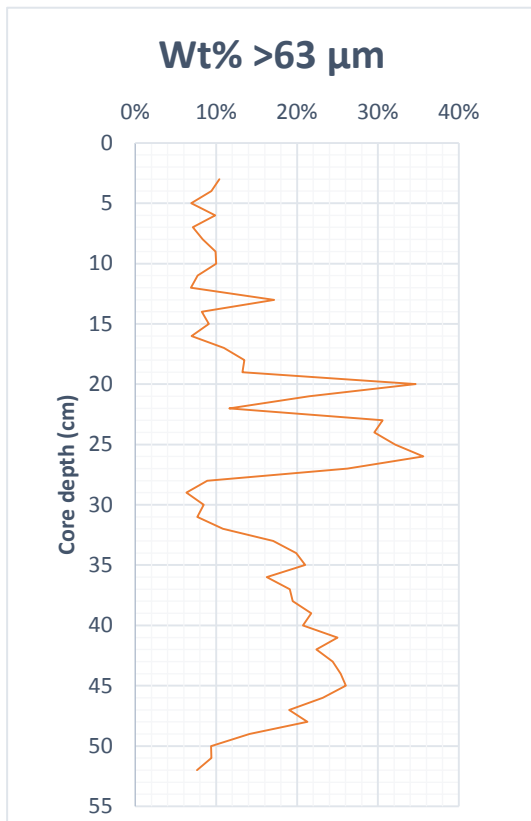


Figure 6. The weight percentage of >63 μm for the sieved samples.

The graph (fig. 6) of the weight percentage show large variations. For the top three samples, between core depth 0 cm and core depth 2 cm no data was obtained, see Appendix.

Several abrupt changes occurs from 14 cm down to 35 cm. One major abrupt change occurs at 20 cm where the concentration goes from being 13% (19 cm) to being almost 35% (20 cm).

Following that a major decrease occurs between 20 cm and 22 cm (down to ca. 12%).

However, an abrupt increase follows, reaching almost 30% at 24 cm. The largest and most abrupt variation occurs between 26 cm and 30 cm. Here, the concentration drops from being about 36% to ca. 8%.

From 30 cm to 35 cm the concentration goes from being 8% to being about 21%. Following that, no major variations occurs down to 45 cm where the concentration is about 26%.

However, a significant decrease occurs that goes to the bottom of the core, where the concentration reaches its lowest value (<8%).

3.2 Bulk analysis

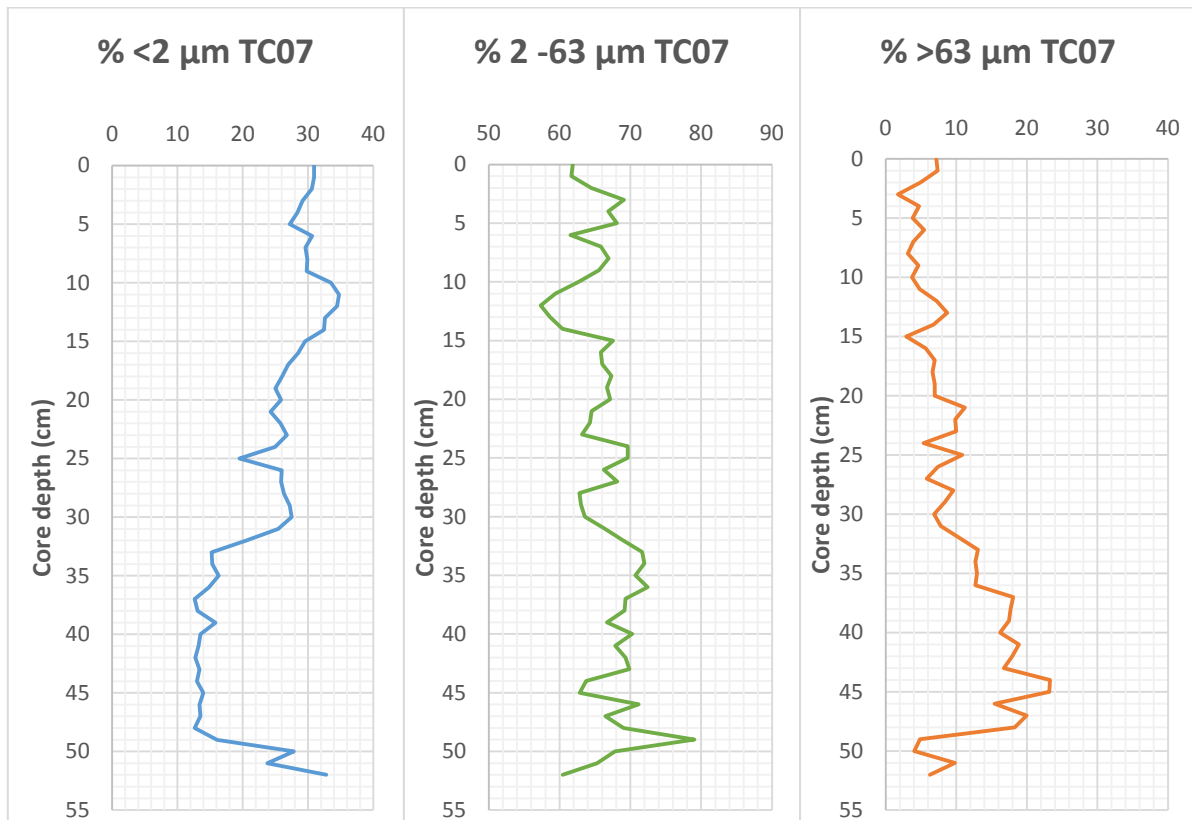


Figure 7. Results from the Malvern Grain Size analyzer over the bulk samples.

Unlike the graphs from the sieved samples, the graphs from the TC 07 bulk analysis (fig.7) do not show a clear tendency in relation to one another. Although the graph over the $<2 \mu\text{m}$ grain size show an approximate opposite tendency at some depths in relation to the $>63 \mu\text{m}$ graph.

3.2.1 Grain size $<2 \mu\text{m}$ TC 07

The $<2 \mu\text{m}$ graph show in general a decrease in concentration from the top of the core down to 49 cm. Between 0 cm and 5 cm a gradual decrease is seen, followed by a slight increase at 6 cm. From 6 cm down to 9 cm no variation occurs, however, an increase in concentration from almost 30% to ca. 34% occurs at 12 cm. After that a gradual decrease in concentration happens down to 20 cm. An abrupt variation occurs at 25 cm, here, the concentration drops from having being almost 25% to 20%, and this is followed by an equal increase in concentration. At 26 cm, the concentration is about 26%. A minor increase occurs towards 30 cm, where the concentration increase with about two percentage points. Between 31 cm and 35 cm, an abrupt decrease occurs down to ca. 15%. From 35 cm down to 41 cm, some fluctuations are seen, followed by minor variations down to 48 cm. From this depth down to 52 cm, a perceptible increase in concentration occurs, from about 16% to almost 33%, however, this increase is interrupt by a relative small decrease that occurs at 51 cm.

3.2.2 Grain size 2-63 μm

The graph of the 2-63 μm show various abrupt variations in concentration. In general is the concentration between 60% and 70%. At four occasions is the concentration either higher or lower. They occur between 11 cm and 14 cm, here, is the concentration less than 60%, reaching its lowest concentration at 13 cm where it is $<59\%$.

The other intervals have concentrations higher than 70%, those are between 33 cm and 38 cm (highest concentration is <73%), at 46 cm (71%), and at 49 cm, where the concentration has abruptly increased to ca. 79%, which also represent the highest concentration. Following this abrupt increase, the most abrupt decrease occurs between 49 cm and 52 cm where the concentration drops to ca. 60%.

3.3.3 Grain size >63 μm

The concentration in >63 μm is in general less than 10% through the core. It is higher between 32 cm and 48 cm. This curve, as mentioned earlier show an approximate opposite tendency to the <2 μm curve. The highest concentration occurs at 45 cm where it is about 23%, whereas the lowest concentration occurs near the top (at 3 cm), where it is <2%. This curve do not show any major abrupt increases, however, a significant decrease occurs between 48 cm and 49 cm, here, the concentration drops from ca.18% to <5%.

3.3 Grain Size results in Piston core 07

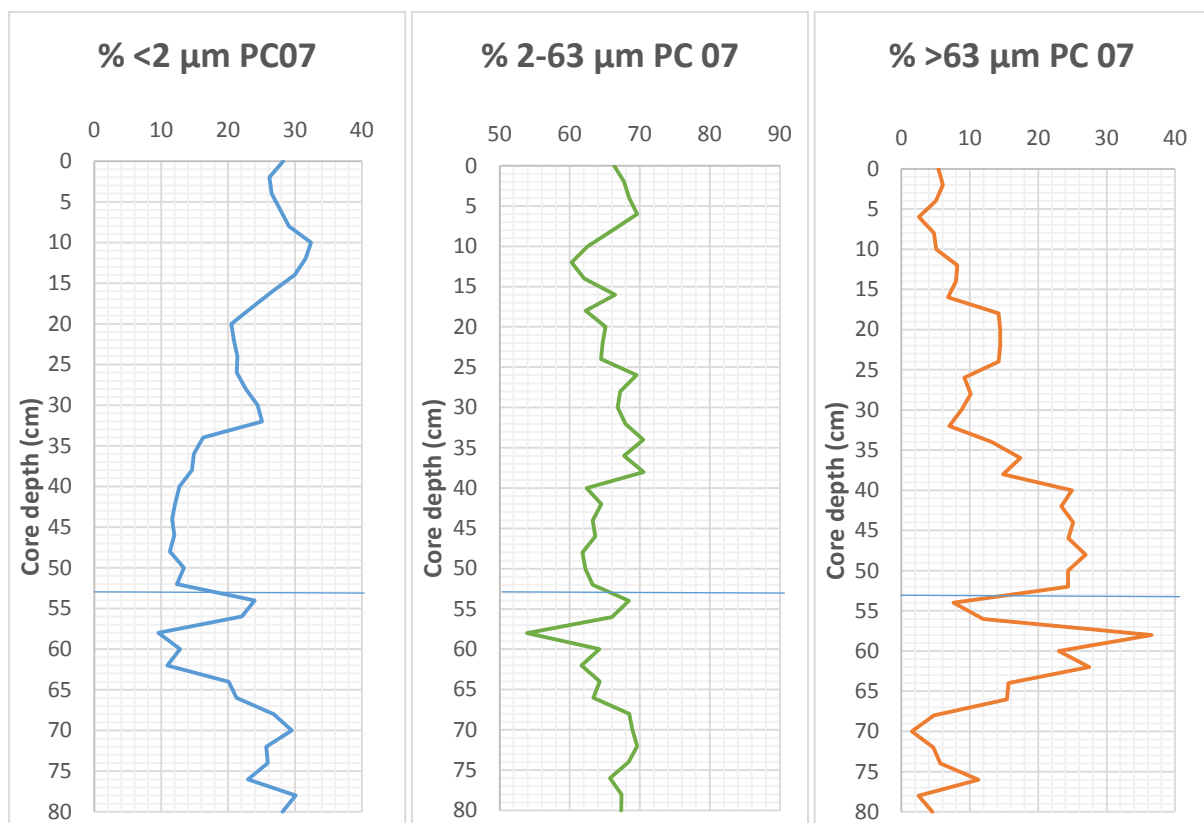


Figure 8. The grain size distribution of the three intervals <2 μm , 2-63 μm , and >63 μm in PC 07. The lines drawn in the graph mark 53 cm in core depth, which correspond with the lowest core depth in TC 07.

The measurements on piston core 07 were made by the scientific party of LOMROG III, the samples were taken every second cm. Most notable variations in concentration occurs in the >63 μm (fig.8), this curve although displaying many fluctuations show an opposite tendency to the <2 μm graph. From the top of the core, down to 5 cm a minor decrease happens in concentration, this is followed by an increase in concentration all the way down to 14 cm. A minor decrease in concentration occurs, followed by an abrupt increase that goes from <7% to ca. 14%. Between 18 cm and 24 cm is the concentration more or less the same before dropping to 9% at 28 cm.

A slight increase occurs at 30 cm (10%) before a decrease down to <7% is seen at 32 cm. From 32 cm to down to 52 cm a general increase in concentration occurs with minor variations in between. Following this increase, several abrupt changes are seen. The first happens between 52 cm and 54 cm, here, the concentration drops from ca. 24% to near 8%, and this is followed by the most significant increase. From 8% at 54 cm to almost 37% at 58 cm. However, a distinguishable decrease (with some minor concentration increases in between) follows the significant increase, and at 70 cm is the concentration <2%, which represent the lowest value of this decrease. From 70 cm to 76 cm an increase to ca.11% occurs before a decrease to <5% happens at 80 cm.

3.4 Correlation of TC 07 and PC 07

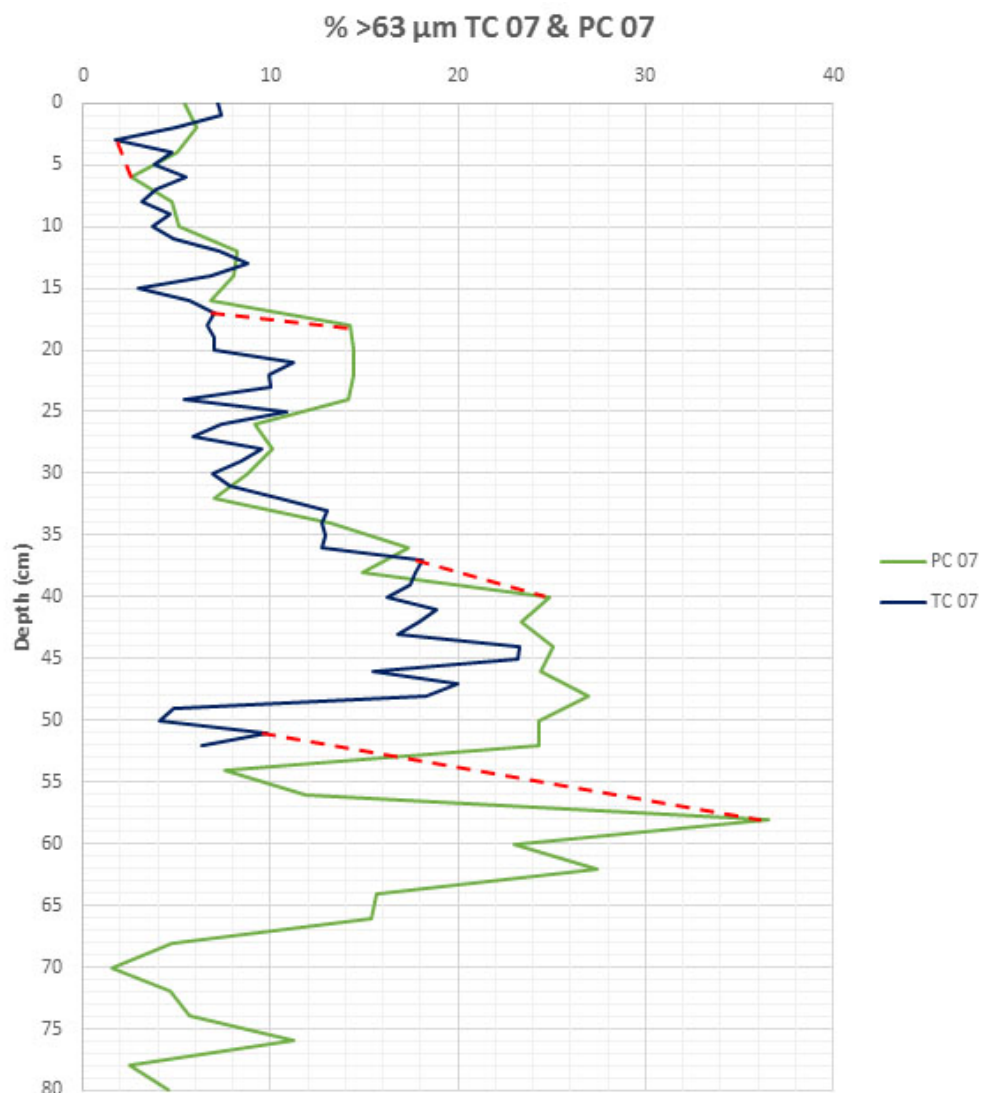


Figure 9. The correlation of TC 07 >63 μm and PC 07 section 1 >63 μm .

The graph for the core correlation between TC 07 and PC 07 <63 μm (fig.9) show that both curves follow the same tendency from the top of the cores down to the bottom of TC 07 at 52 cm, although PC 07 is slightly displaced downwardly in relation to TC 07.

Four dashed lines mark four different points where the curves clearly follow the same tendency. The lowest point in TC 07 where a dashed line was drawn to correlate with PC 07 is at 51 cm, which corresponds to 57 cm in PC 07.

3.5 Correlation of PC 07 and ACEX

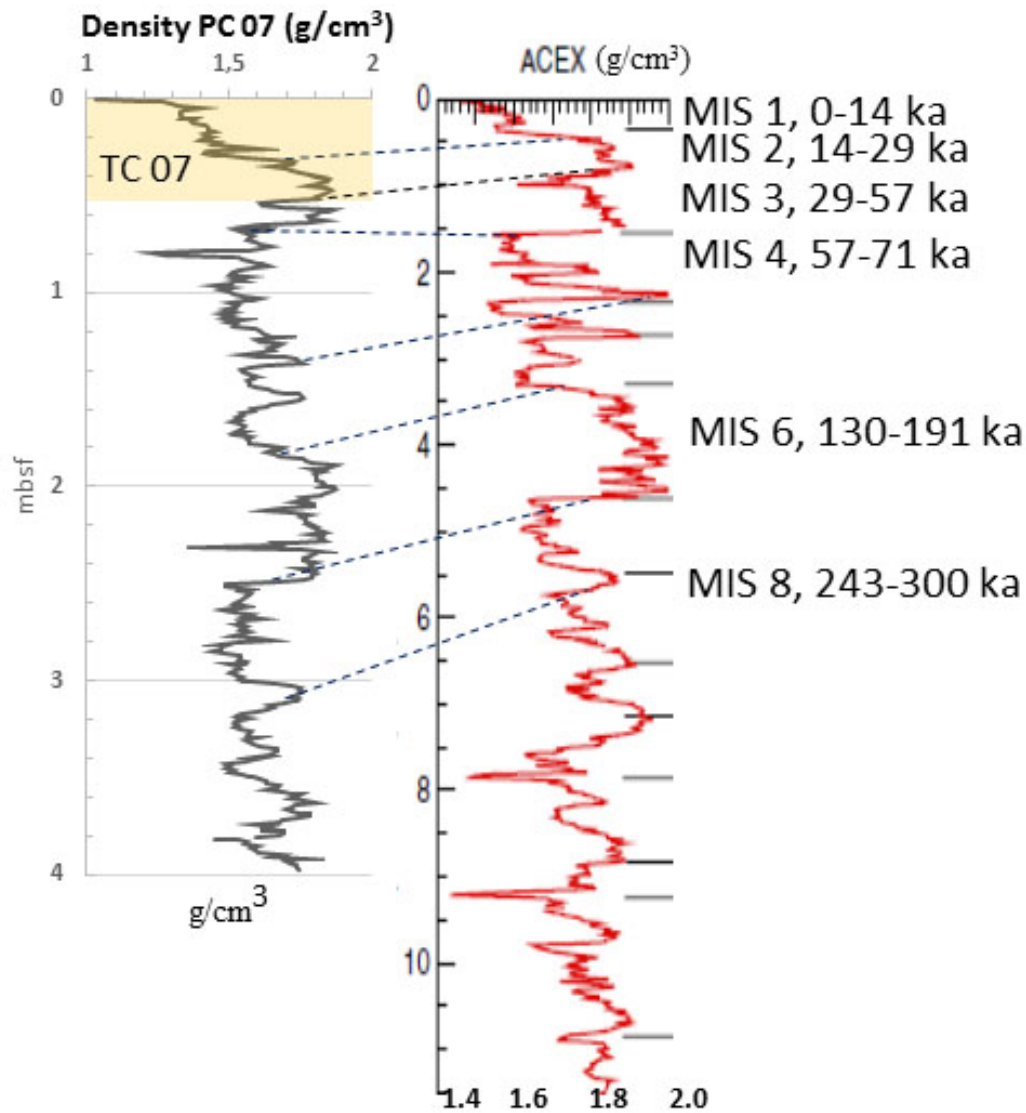


Figure 10. Correlation of PC 07 density and ACEX density (taken and modified from O'Regan et al., 2014). Dashed lines are drawn where the curves are interpreted to correlate with one another, and the yellow area at the top of PC 07 show TC 07 depth in relation to PC 07. MIS boundaries, at the right side of the ACEX curve show age scale for the curves.

Seven dashed lines are drawn from PC 07 and ACEX for correlation (fig.10). The first correlation is at ca. 35 cm in PC 07, which in TC 07 is ca. 32 cm and represents the beginning of MIS 2. A second line is drawn at a point which is close to the bottom of TC 07 and represents the beginning of MIS 3. PC 07 show similarities to ACEX, however, the dashed lines are in a lower core depth in ACEX suggesting that there are higher sedimentation rates at the location of where ACEX is collected in relation to the location of where PC 07 and TC 07 are collected.

4 Discussion

4.1 Methodology

Two different approaches were done for the purpose of measuring the grain size in TC 07. In the first approach, the samples were subsampled, wet-sieved, dried, and measured in the Malvern grain size analyzer, while in the second approach the samples were directly taken from the core and measured in the Malvern grain size analyzer. Measuring the grain size by doing two different approaches gives a better understanding, but also, for the intention to compare which is more effective.

The purpose of doing pre-work on the first approach was to divide the fine-grained sediment ($<63\ \mu\text{m}$) and the coarse-grained sediment ($>63\ \mu\text{m}$). This approach was not done by the Oden scientific party on PC 07 and the other collected cores, instead they applied the second mentioned approach, which was to take the sediment directly from the core.

Some difficulties with the first approach delayed the measurements and analysis.

0.5% Sodiumhexametaphosphate, Calgon, was used in wet sieving as a dispersion solution, however, the can that contained the solution laid next to the can that contained Calgon but with 10% concentration, that is to say 200 times higher concentration.

This created complications, as they were confused and between cm ~ 20 and ~ 40 cm they were both used. Naturally, it delayed the drying in the oven because the higher concentration of Calgon created large crystals in both the dried samples with $>63\ \mu\text{m}$ and $<63\ \mu\text{m}$. To get around this problem, the samples that contained $<63\ \mu\text{m}$ were diluted with deionized water. The samples with the right concentration dried after approximately 3 days, whereas the samples with the higher concentration needed more than 7 days of drying, simultaneously treated with deionized water as earlier mentioned. The deionized water was siphoned out. The samples were not measured in the correct order as they were intended to in the Malvern grain size analyzer, but, as they dried.

Assuming that this problem would not have happened, this approach would have been effective. However, direct measurements from the core are more time saving, but, a problem that can emerge with this approach is that one might not get a representative result if a single-large grain happens to be picked up and measured by the Malvern grain size analyzer. One problem with the Malvern Grain Size analyzer though, is that when the data is exported into Excel, and the mean value is going to be calculated for $<2\ \mu\text{m}$ to give an example, the bin size is set to select either $1.88\ \mu\text{m}$ or $2.13\ \mu\text{m}$ because the bin size of $2\ \mu\text{m}$ does not exist. The same issue is with $2-63\ \mu\text{m}$ and $>63\ \mu\text{m}$, where the bin size is $58.9\ \mu\text{m}$ or $66.9\ \mu\text{m}$, however after testing with all grain size intervals, the mean value does not vary significant. For this study, $2.13\ \mu\text{m}$ and $66.9\ \mu\text{m}$ were selected.

4.2 Sieved sampling analysis

Using the wrong concentration of dispersion solution had a clear effect on the results from the pre-worked samples. The first two graphs, $<2\ \mu\text{m}$ and $2-63\ \mu\text{m}$ (fig.5), show an opposite tendency to one another, while the third graph, $>63\ \mu\text{m}$ (fig.5), which should be 0, has concentrations of up to 6%. This is probably because of aggregation of grains and large crystals that were not dispersed before being measured in the Malvern grain size analyzer. An interesting observation is that the curve for wt.% $>63\ \mu\text{m}$ (fig.6) seems to follow an approximate similar tendency to the $2-63\ \mu\text{m}$ (fig.5). It is clear in the wt% curve that it show large variations between 20 cm and 40-45 cm, and this is corroborated with large crystals that formed in this interval due to the high concentrations of Calgon.

The top unit in the core (fig.3), which goes from the top of the core down to 32 cm, is mostly brown, which according to Löwemark *et al.* (2014) is characteristic of interglacial periods with high amounts of manganese, Mn, but also of fine-grained material (Jakobsson *et al.*, 2014). This can be related to the decrease in the graph of 2-63 μm (fig.5) between the top of the core down to ca. 15 cm, after that an significant increase in concentration is seen in the graph with several abrupt changes that can probably be related to the higher concentrations of Calgon. However, at the bottom of unit 1 (32 cm), the grain size increases, although some fluctuations are seen in the 2-63 μm graph (fig.5). This increase can be associated to the grayish-yellow-beige colored unit that is described as glacial deposits with coarser grain size (Jakobsson *et al.*, 2000). According to Sellén *et al.* (2008), coarse-grained material is related to iceberg discharge and sea ice-rafting.

In the preliminary core description, two units were described between 32 cm and 49 cm, one at 32 cm, and only 1-cm-wide, and the second from 33 cm down to 49 cm. These two units are probably one whole unit, although a sharp contact surface is located at 33 cm, this is probably because the glacial period was ending. At 50 cm in the 2-63 μm graph (fig.5) , a significant decrease in grain size occurs, this is related to the end of unit two in the core. Finer grains are more abundant, and the color is more gray-brown, which can be interpreted as interglacial deposits. The last two units in the core, at 51 cm, and at 52 cm, are olive-brown respectively dark brown. These two units have coarser grain size in relation to unit 3, however, they are interpreted to be interglacial deposits with high amounts of Mn and low amount of coarse material.

It is difficult to interpret glacial and interglacial periods based on the wt% >63 μm graph (fig.6), and that is because of large variations in the curve, probably because of large crystals that formed due to the wrong concentration of dispersion solution. However, between 3 cm and 16 cm (ignoring the abrupt change occurring at 13 cm) is the wt% low, as it should be during interglacial periods. Following, down to 40-45 cm is the curve unreliable, and therefore it is difficult to make an interpretation for the rest of the core.

4.3 Bulk analysis

The bulk measurements were taken directly from the sediment core every cm. Unlike the sieved samples, no problems emerged during this approach. The graph of >63 μm (fig.7), which also is selected for correlation with piston core 07, show numerous fluctuations, however, in general the concentration lays between 2% and 10% from the top of the core down to 30 cm, and this can be associated with the brown color unit in the core (fig.3). As mentioned earlier, they are interpreted to represent interglacial deposits. After that an increase of coarse material begins, and at 33 cm is the concentration 13%. Between 33 cm and 48 cm a general increase of coarser material is seen. This can be associated with the grayish-beige color in the core, which also corresponds with the general increase in concentration of coarse material in the 2-63 μm graph (sieved samples, fig.5). This supports the claim that unit 2 are glacial sediments. An interesting remark is that like the 2-63 μm graph (sieved samples, fig.5) and the wt% >63 μm (fig.6), the >63 μm graph (fig.7) also shows a decrease at 49-50 cm. This is probably, as mentioned earlier when the glacial period began (as the bottom sediments are older than the top sediments).

4.4 Chronology of TC 07

The discussed graphs in the subheadings 4.2 and 4.3, supports that the top unit, that goes down to ca. 32 cm is an interglacial deposit.

This unit is characterized by finer particles and brown in color (Mn-enriched). The second unit (~32 cm to -49 cm), gray-beige colored, and with coarser material (seen in the 2-63 μm sieved sample graph, fig.5, and in the >63 μm bulk sample graph, fig.6) can be interpreted as glacial deposits. The last three units, 50 cm, 51 cm, and 52 cm, although they show sharp contact surface to one another, are probably interglacial deposits. All three units show less amounts of coarse material (fig.7), and are brown in color with different shades. The correlation with piston core 07 (fig.9) also supports the claim that between 0 cm and 32 cm, the sediments are interglacial, followed by glacial deposits down to 49 cm, ending with interglacial deposits. Four dashed lines are drawn between both graphs to show where the interpreted correlations occur. Although, the curves are unequally displaced, they follow a similar tendency. The displacement of the curves in relation to one another is because TC 07 is a gravity core, meaning that it is shorter and that it free-falls into the sediment before the piston core, PC 07. The piston core is triggered when the gravity core hits the sea-floor. Also, the samples taken in TC 07 are taken every cm, while in PC 07, the samples are taken every second cm.

According to Moran *et al.* (2006) the coarsening of sediments increases the bulk density, which are interpreted as greater input of ice-rafted debris during glacial periods. This can be seen in the correlation of PC 07 density curve and ACEX (fig.10). An increase in density occurs at ~30-35 cm. At ca. 50 cm in PC 07, a drop in density occurs, which correlates with the drop of coarse material at 49 cm in TC 07.

Two dashed lines are drawn from PC 07 to ACEX at depths of ~38 cm and ~48 cm. These two lines represent unit 1 in TC 07 where the coarser material is present, also, it can be related to Marine Isotope Stage 2, or MIS 2 (fig. 10). Following this claim, the top of TC 07 can be attributed to MIS 1, whereas the bottom of the core, could be the boundary of MIS 2/MIS 3. Applying a constant sedimentation rate of 1.5 cm/1000 years on TC 07 (Gard 1993, Backman *et al.*, 2004), gives the bottom of the core an age of ~36000 years. Following this claim, the gray-beige unit (~32~49 cm), which is interpreted as a glacial deposit, gives an age to this interval of ~21000 years and ~33000 years. This supports the claim that these sediments were deposited during the MIS 2, which represent the LGM (Last Glacial Maximum).

5 Conclusions

Based on the approaches, the results, and the scientific literature, the following conclusions can be drawn for this study;

1. The approach of taking the samples directly from the sediment core for grain size analysis is more effective and more time saving than doing pre-work on the sediment.
2. Trigger core 07, TC 07, from the Lomonosov Ridge in the central Arctic Ocean contain interglacial and glacial sediments.
3. From the top of the core down to 32 cm in core depth, the sediments are fine-grained, brown colored due to an enrichment in manganese, Mn, which is typical of interglacial sediments. These sediments can be linked to MIS 1, Marine isotope Stage 1.
4. The following sediments, which are between 32 cm and 49 cm in core depth, are coarser-grained, gray-beige in color, which characterizes glacial sediments. These sediments can be linked with MIS 2, and the LGM, (Last Glacial Maximum), which lasted between ~19000 years ago and ~26000 years ago.

6 Acknowledgements

I would like to thank the Department of Geological Sciences at Stockholm University for their support and specially my supervisor Dr. Richard Gyllencreutz for his help, expertise and guidance through the whole project, Therese Granberg for her great help with the Malvern grain size analyzer, and Carina Johansson for her support in the laboratory.

Special thanks to Ernesto Fuentes for his help with Excel, Raquel Guerrero for her support through the project, and Carolina Serain Aranis for her help with the structure of the thesis. I would also like to thank my siblings, Emely and Daniel, my nephew William, my brother in law Oscar, and my lovely Chow Chow, Dina for their care and for their interest shown in my thesis and my education.

7 References

7.1 Articles

Backman, J., Jakobsson, M., Løvlie, R., Polyak, L. & Febo, L.A. (2004). Is the central Arctic Ocean a sediment starved basin? *Quaternary Science Reviews* **23**, 1435-1454.

Björk, G., Jakobsson, M., Rudels, B., Swift, J.H., Anderson, L., Darby, D.A., Backman, J., Coakley, B., Winson, P., Polyak, L. & Edwards, M. (2007). Bathymetry and deep-water exchange across the central Lomonosov Ridge at 88-89°N. *Deep-Sea Research I* **54**, 1197-1208.

Chanell, J.E.T. & Xuan, C. (2009). Self-reversal and apparent magnetic excursions in the Arctic sediments. *Earth and Planetary Science Letters* **284**, 124-131.

Clark, P.U., Dyke, A.S., Shakun, J.D., Carlson, A.E., Clark, J., Wohlfarth, B., Mitrovica, J.X., Hostetler, S.W. & McCabe, A.M. (2009). The Last Glacial Maximum. *Science* **325**, 710-714.

Darby, D.A. (2003). Sources of sediment found in sea ice from western Arctic Ocean, new insights into processes of entrainment and drift patterns. *Journal of Geophysical Research* **108**.

Gard, G. (1993). Late Quaternary coccoliths at the North Pole: evidence of ice-free conditions and rapid sedimentation in the central Arctic Ocean. *Geology* **21**, 227-230.

Hölemann, J.A., Schirmacher, M. & Prange, A. (2005). Seasonal variability of trace metals in the Lena River and the southeastern Laptev Sea: Impact of the spring freshet. *Global and Planetary Change* **48**, 112-125.

Jakobsson, M., Løvlie, Al-Hanbali, H., Arnold, E., Backman, J. & Mörth, M. (2000). Manganese and color cycles in Arctic Ocean sediments constrain Pleistocene chronology. *Geology* **28**, 23-26.

Jakobsson, M., Løvlie, R., Arnold, E.M., Backman, J., Polyak, L., Knutsen, J.-O. & Musatov, E. (2001). Pleistocene stratigraphy and paleoenvironmental variation from Lomonosov Ridge sediments, central Arctic Ocean. *Global and Planetary Change* **31**, 1-22.

Jakobsson, M., Polyak, L., Edwards, M., Kleman, J. & Coakley, B. (2008). Glacial geomorphology of the Central Arctic Ocean: the Chukchi Borderland and the Lomonosov Ridge. *Earth Surf. Process. Landforms* **33**, 526-545.

- Jakobsson, M., Andreassen, K., Bjarnadóttir, L.R., Dove, D., Dowdeswell, J.A., England, J.H., Funder, S., Hogan, K., Ingólfsson, Ó., Jennings, A., Larsen, N.K., Kirchner, N., Landvik, J.Y., Mayer, L., Mikkelsen, N., Möller, P., Niessen, F., Nilsson, J., O'Regan, M., Polyak, L., Nørgaard-Pedersen, N. & Stein, R. (2014). Arctic Ocean glacial history. *Quaternary Science Reviews* **92**, 40-67.
- Lisiecki, L. & Raymo, M.E. (2005). A Pliocene- Pleistocene stack of 57 globally distributed benthic $\delta^{18}\text{O}$ records. *Paleoceanography* **20**, PA1003. doi: 10.1029/2004PA001071.
- Löwemark, L., März, C., O'Regan, M. & Gyllencreutz, R. (2014). Arctic Ocean Mn-stratigraphy: genesis, synthesis and inter-basin correlation. *Quaternary Science Reviews* **92**, 97-111.
- Macdonald, R. & Gobeil, C. (2012). Manganese sources and sinks in the Arctic Ocean with reference to Periodic enrichments in basin sediments. *Aquatic Geochemistry* **18**, 565-591.
- Marcussen, C. and the LOMROG III Scientific Party. (2012). Lomonosov Ridge off Greenland 2012 (LOMROG III) - Cruise Report. Danmarks og Grønlands Geologiske Undersøgelse Rapport 2012/119.
- Minakov, A.N. & Podladchikov, Y.Y. (2012). Tectonic subsidence of the Lomonosov Ridge. *Geology* **40**, 99-102.
- Moran, K., Backman, J. & the IODP Expedition 302 Scientific Party. (2006). The Cenozoic paleoenvironment of the Arctic Ocean. *Nature* **441**, 601-605.
- O'Regan, M., King, J., Backman, J., Jakobsson, M., Pälike, H., Moran, K., Heil, C., Sakamoto, T., Cronin, T.M. & Jordan, R.W. (2008). Constraints on the Pleistocene chronology of sediments from the Lomonosov Ridge. *Paleoceanography* **23**, PA1S19.
- O'Regan, M., Sellén, E. & Jakobsson, M. (2014). Middle to late Quaternary grain size variations and sea-ice rafting on the Lomonosov Ridge. *Polar Research* **33**, 23672.
- Polyak, L., Best, K.M., Crawford, K.A., Council, E.A. & St-Onge, G. (2013). Quaternary history of sea ice in the western Arctic Ocean based on foraminifera. *Quaternary Science Review* **79**, 145-156.
- Sellén E., Jakobsson M., Backman, J. (2008). Sedimentary regimes in Arctic's Amerasian and Eurasian Basins: Clues to differences in sedimentation rates. *Global and Planetary Change* **61**, 275-284.
- Shephard, G.E., Müller, R.D., & Seton, M. (2013). The tectonic evolution of the Arctic since Pangea breakup: Integrating constraints from surface geology and geophysics with mantle structure. *Earth Science- Review* **124**, 148-183.
- St. John, K. (2008). Cenozoic ice-rafting history of the central Arctic Ocean: Terrigenous sands on the Lomonosov Ridge. *Paleoceanography* **23**, PA1S05.
- Strand, K., Immonen, N. (2010). Dynamics of the Barents-Kara ice sheet as revealed by quartz sand grain microtextures of the late Pleistocene Arctic Ocean sediments. *Quaternary Science Review* **29**, 3583-3589.
- Timermans, M.-L., Winson, P. & Whitehead, J.A. (2005). Deep-Water Flow over the Lomonosov Ridge in the Arctic Ocean. *Journal of Physical Oceanography* **35**, 1489-1493.

Verzhbitskii, E.V., Lobkovskii, L.I., Byakov, A.F. & Kononov, M.V. (2012). The Origin and Age of the Alpha-Mendeleev and Lomonosov Ridges in the Amerasian Basin. *Oceanology* **53**, 89-98.

7.2 Books

McManus, J. (1988). *Techniques in Sedimentology*. Eds. Tucker, M. London: Blackwell Science Ltd. p63-85.

7.3 Internet references

Geology.com- Arctic Ocean

<http://geology.com/articles/arctic-ocean-features/> Last accessed 2015-05-30.

Integrated Ocean Drilling Program, Expedition 302 Preliminary Report. Arctic Coring Expedition (ACEX). Paleooceanographic and tectonic evolution of the central Arctic Ocean. http://publications.iodp.org/preliminary_report/302/302PR.PDF Last Accessed 2015-06-02

Lorraine Lisiecki's Homepage

<http://www.lorraine-lisiecki.com/stack.html> Last accessed 2015-06-04

Malvern Webpage Mastersizer 3000.

<http://www.malvern.com/en/products/product-range/mastersizer-range/mastersizer-3000/default.aspx>. Last accessed 2015-05-02.

8 Appendix

The table show the subsampling data.

Core depth (cm)	Weighing boat (g)	Weighing boat with sediment (g)	Sediment weight (g)	>63 μ m weight	Wt% >63 μ m
0			0	0,8142	
1			0	0,7684	
2			0	0,7574	
3	0,641	8,193	7,552	0,7864	0,104
4	0,628	8,955	8,327	0,7832	0,094
5	0,615	12,711	12,096	0,8387	0,069
6	0,587	7,819	7,232	0,7137	0,099
7	0,577	11,190	10,613	0,7557	0,071
8	0,624	10,147	9,523	0,7948	0,083
9	0,637	8,508	7,871	0,7823	0,099
10	0,627	12,04	11,413	1,1401	0,100
11	0,632	11,124	10,492	0,81	0,077
12	0,592	11,939	11,347	0,7821	0,069
13	0,651	10,386	9,735	1,672	0,172
14	0,646	18,156	17,51	1,44	0,082
15	0,58	9,919	9,339	0,8494	0,091
16	0,658	15,014	14,356	0,9983	0,070
17	0,606	15,014	14,408	1,5781	0,110
18	0,621	19,163	18,542	2,4972	0,135
19	0,574	24,291	23,717	3,1391	0,132

20	0,596	5,509	4,913	1,702	0,345
21	0,604	10,65	10,046	2,1612	0,215
22	0,615	11,709	11,094	1,2911	0,117
23	0,65	14,482	13,832	4,231	0,306
24	0,611	15,2	14,589	4,312	0,296
25	0,606	16,863	16,257	5,221	0,321
26	0,589	15,504	14,915	5,312	0,356
27	0,575	14,769	14,194	3,721	0,262
28	0,583	10,666	10,083	0,8966	0,089
29	0,594	15,138	14,544	0,9202	0,063
30	0,615	10,862	10,247	0,8665	0,085
31	0,619	12,304	11,685	0,898	0,077
32	0,589	11,529	10,94	1,185	0,108
33	0,607	14,155	13,548	2,308	0,170
34	0,611	13,868	13,257	2,637	0,199
35	0,609	13,102	12,493	2,626	0,210
36	0,665	10,293	9,628	1,564	0,162
37	0,66	11,907	11,247	2,15	0,191
38	0,668	18,067	17,399	3,383	0,194
39	0,57	16,144	15,574	3,39	0,218
40	0,623	16,377	15,754	3,267	0,207
41	0,655	15,868	15,213	3,801	0,250
42	0,628	17,705	17,077	3,824	0,224
43	0,631	11,551	10,92	2,664	0,244
44	0,621	13,196	12,575	3,192	0,254
45	0,64	16,271	15,631	4,071	0,260
46	0,601	12,316	11,715	2,715	0,232
47	0,612	14,659	14,047	2,673	0,190
48	0,594	13,792	13,198	2,811	0,213
49	0,617	9,971	9,354	1,321	0,141
50	0,581	9,733	9,152	0,857	0,094
51	0,631	9,642	9,011	0,847	0,094
52	0,627	13,277	12,65	0,963	0,076